Dynamical control of pulse propagation in electromagnetically induced transparency

Martin Kiffner[1,*] and T. N. Dey[1,2,†]
[1]*Max-Planck-Institut für Kernphysik, Saupfercheckweg 1, 69117 Heidelberg, Germany*
[2]*Indian Institute of Technology Guwahati, Guwahati, 781 039 Assam, India*
(Received 17 June 2008; published 24 February 2009)

The influence of a phase-modulated control field on the phenomenon of electromagnetically induced transparency (EIT) is investigated theoretically. We show that the phase modulation changes the dispersive properties of the medium considerably since it results in temporal oscillations of the transparency window in frequency space. This is in marked contrast to the standard EIT setup, where the transparency window is fixed and determined by the two-photon resonance condition. In particular, we find that the phase modulation enables the propagation of probe pulses with disjoint frequency spectra at different times and allows the shifting of the central frequency of a probe pulse almost without distortion of its shape. We employ the time-dependent susceptibility of the medium to explain and analyze our results and demonstrate that this concept yields qualitative as well as quantitative agreement with the numerical integration of Maxwell-Bloch equations. Our theoretical model can be applied to other media with time-dependent susceptibilities.

DOI: 10.1103/PhysRevA.79.023829 PACS number(s): 42.50.Gy, 32.80.Qk, 42.65.−k

I. INTRODUCTION

One of the most intriguing phenomenon in atom-light interactions is represented by electromagnetically induced transparency (EIT). Since the prediction [1] and first observation [2] of this effect, EIT triggered various exciting developments that are relevant, e.g., for the fields of nonlinear optics and quantum information theory [3–5]. Prominent examples are given by the slowing and stopping of light [6–8] as well as the coherent storage and retrieval of light [9–13]. Furthermore, it has been shown that EIT can be employed to generate giant optical nonlinearities [14–18] that enable light-light interactions.

The generic EIT scheme [4] consists of a gas comprised of three-level atoms in Λ configuration that are driven by a strong control field and a weak probe field on separate transitions. If the frequencies of the probe and control fields are in two-photon resonance, the atoms are driven into a so-called dark state that is decoupled from the light fields. This mechanism creates a transparency window in the absorption spectrum of the probe field, and the steep normal dispersion at the center of the dip in the absorption spectrum results in small group velocities for probe pulses.

Slow light in a generic EIT medium is constrained by several conditions. First of all, the lossless propagation of a probe pulse without distortion of its shape requires that its Fourier components are well contained within the transparency window [19]. Note that the position of the transparency window in frequency space is fixed for a given setup and determined by the two-photon resonance condition. Furthermore, extremely slow group velocities that result in long-time delays are particularly relevant for applications but can only be achieved for narrow-band probe pulses.

In order to overcome some of these limitations, modifications of the usual EIT setup have been suggested. For example, two different schemes discuss the possibility to achieve slow light for broadband pulses [20–23]. The first approach [20,22] is based on a spatial separation of the Fourier components of the broadband pulse and a subsequent delay of the individual components by appropriately tuned EIT systems. A proof-of-principle experiment in room-temperature solids was reported in [21]. In the second approach [23], transparency for a broadband pulse with large time delay is achieved by matched pairs of probe and control field Fourier components that individually obey the two-photon resonance condition.

In this paper, we modify the generic EIT setup by the application of a phase-modulated control field and demonstrate that this alteration allows the relaxation of the two-photon resonance condition considerably. More specifically, it is found that the phase modulation gives rise to periodic changes in the position of the transparency window in frequency space. This enables the propagation of probe pulses with disjoint frequency spectra at different times. Furthermore, our scheme can be employed to shift the central frequency of a probe pulse without significant distortion of its shape. It follows that our findings extend and enhance the potential of EIT media for the purpose of signal processing. For the explanation of our results, we put forward the concept of time-dependent susceptibilities that also applies to other systems.

The organization of the paper is as follows. In Sec. II, we introduce the coupled set of Maxwell-Bloch equations governing the dynamics of the optical fields and the atomic degrees of freedom. In Sec. III, we present the results of numerical integrations of Maxwell-Bloch equations for different incoming probe fields. A theoretical model for the system under consideration is established in Sec. IV. In particular, the linear response of the medium to the probe field is studied in terms of a time-dependent susceptibility in Sec. IV A. We then employ this concept to explain the essential features of the numerical results, see Sec. IV B. The influence of the phase modulation on the probe field in frequency space is analyzed in Sec. IV C. Here we also recover the numerical results for the propagation of the probe field

*martin.kiffner@ph.tum.de
†tarak.dey@gmail.com

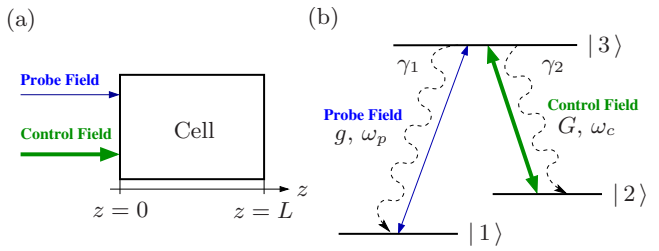

FIG. 1. (Color online) (a) Schematic setup of the system of interest. The atomic gas extends from $z=0$ to $z=L$ and is driven by two classical laser fields $\boldsymbol{E}_c$ and $\boldsymbol{E}_p$. (b) The atomic gas is comprised of three-level atoms in Λ configuration with excited state $|3\rangle$ and ground states $|1\rangle$ and $|2\rangle$. The phase-modulated control field $\boldsymbol{E}_c$ couples to the transition $|3\rangle\leftrightarrow|2\rangle$, and the probe field $\boldsymbol{E}_p$ interacts with the $|3\rangle\rightarrow|1\rangle$ transition. The spontaneous emission rate on the $|3\rangle\rightarrow|i\rangle$ transition is γ_i $(i\in\{1,2\})$.

within the framework of the linear theory. Finally, a summary and discussion of our results is presented in Sec. V.

II. MAXWELL-BLOCH EQUATIONS

The physical system under consideration is an isotropic homogeneous atomic gas driven by two laser fields that propagate in z direction, see Fig. 1(a). The probe field $\boldsymbol{E}_p$ is defined by

$$\boldsymbol{E}_p(z,t)=\boldsymbol{E}_p^{(+)}(z,t)+\text{c.c.}, \tag{1a}$$

$$\boldsymbol{E}_p^{(+)}(z,t)=\boldsymbol{e}_p\mathcal{E}_p(z,t)e^{-i\omega_p(t-z/c)}, \tag{1b}$$

and its positive frequency part $\boldsymbol{E}_p^{(+)}$ is characterized by the unit polarization vector $\boldsymbol{e}_p$, central frequency ω_p, and envelope function $\mathcal{E}_p$. The second field is the control field $\boldsymbol{E}_c$ with unit polarization vector $\boldsymbol{e}_c$, central frequency ω_c, and envelope function $\mathcal{E}_c$,

$$\boldsymbol{E}_c(z,t)=\boldsymbol{E}_c^{(+)}(z,t)+\text{c.c.}, \tag{2a}$$

$$\boldsymbol{E}_c^{(+)}(z,t)=\boldsymbol{e}_c\mathcal{E}_c(z,t)e^{-i\omega_c(t-z/c)}. \tag{2b}$$

In the region to the left of the gas cell $(z<0)$, we suppose that the control field is a continuous wave whose phase is modulated with respect to time. The envelope function $\mathcal{E}_c$ at the boundary $z=0$ can thus be written as

$$\mathcal{E}_c(z=0,t)=\mathcal{E}_0e^{-i\varphi(t)}, \tag{3}$$

where $\varphi(t)$ is a real-valued function of time and $\mathcal{E}_0$ is a time-independent constant. In particular, we consider the case where the phase varies sinusoidally with modulation index M and frequency Ω,

$$\varphi(t)=M\sin(\Omega t). \tag{4}$$

It follows that the Fourier series of the periodic exponential in Eq. (3) can be written as

$$e^{-i\varphi(t)}=\sum_{n=-\infty}^{\infty}e^{in\Omega t}J_n(-M), \tag{5}$$

where J_n are Bessel functions. The phase modulation according to Eqs. (3) and (4) thus corresponds to a polychromatic control field where the weight of the frequency component $n\Omega$ is determined by $J_n(-M)$. However, we emphasize that the phase modulation leads to a very special polychromatic field since its intensity is constant in time. This is in contrast to the intensity of an arbitrary polychromatic field that oscillates with the beat note of the involved frequencies, in general.

The level scheme of each atom is a three-level system in Λ configuration, see Fig. 1(b). We assume that the polarization vectors of the two laser fields are chosen such that the probe field $\boldsymbol{E}_p$ interacts with the atomic transition $|1\rangle\leftrightarrow|3\rangle$ and the control field $\boldsymbol{E}_c$ couples to the $|2\rangle\leftrightarrow|3\rangle$ transition. In electric-dipole and rotating-wave approximation, the Hamiltonian of the system is

$$H=-\hbar\omega_{31}|1\rangle\langle 1|-\hbar\omega_{32}|2\rangle\langle 2| -(|3\rangle\langle 1|\boldsymbol{d}_{31}\cdot\boldsymbol{E}_p^{(+)}+|3\rangle\langle 2|\boldsymbol{d}_{32}\cdot\boldsymbol{E}_c^{(+)}+\text{H.c.}), \tag{6}$$

where ω_{3i} denotes the resonance frequency on the transition $|3\rangle\leftrightarrow|i\rangle$ and $\boldsymbol{d}_{3i}=\langle 3|\hat{\boldsymbol{d}}|i\rangle$ is the matrix element of the electric dipole moment operator $\hat{\boldsymbol{d}}$. We describe the time evolution of the atomic system by a master equation for the reduced density operator R,

$$\partial_tR=-\frac{i}{\hbar}[H,R]+\mathcal{L}_\gamma R. \tag{7}$$

The last term in Eq. (7) describes spontaneous emission and is determined by

$$\mathcal{L}_\gamma R=-\sum_{i=1}^{2}\frac{\gamma_i}{2}(S_i^+S_i^-R+RS_i^+S_i^--2S_i^-RS_i^+), \tag{8}$$

where the atomic transition operators are defined as

$$S_i^+=|3\rangle\langle 1|,\quad S_i^-=(S_i^+)^\dagger. \tag{9}$$

While the ground states $|1\rangle$ and $|2\rangle$ are assumed to be (meta)stable, the decay rate of the excited state $|3\rangle$ on the transition $|3\rangle\rightarrow|i\rangle$ is given by $\gamma_i(i\in\{1,2\})$.

For the formulation of the coupled Maxwell-Bloch equations, it is advantageous to transform Eq. (7) into a rotating frame defined by

$$W=\exp[-i(\omega_p|1\rangle\langle 1|+\omega_c|2\rangle\langle 2|)(t-z/c)]. \tag{10}$$

It follows that the transformed density operator $\varrho=WRW^\dagger$ obeys the master equation,

$$\partial_t\varrho=-\frac{i}{\hbar}[H',\varrho]+\mathcal{L}_\gamma\varrho, \tag{11}$$

and the transformed Hamiltonian H' is

$$H'=\hbar\Delta_p|1\rangle\langle 1|+\hbar\Delta_c|2\rangle\langle 2|-\hbar(g|3\rangle\langle 1|+G|3\rangle\langle 2|+\text{H.c.}). \tag{12}$$

In this equation, Δ_p is the detuning of the probe field with the $|1\rangle\leftrightarrow|3\rangle$ transition and Δ_c represents the detuning of the control field with the $|2\rangle\leftrightarrow|3\rangle$ transition,

$$\Delta_p = \omega_p - \omega_{31}, \quad \Delta_c = \omega_c - \omega_{32}. \tag{13}$$

The parameters g and G in the second line of Eq. (12) denote the Rabi frequencies of the probe and control fields, respectively,

$$g = \frac{\boldsymbol{d}_{31}\cdot\boldsymbol{e}_p}{\hbar}\mathcal{E}_p, \quad G = \frac{\boldsymbol{d}_{32}\cdot\boldsymbol{e}_c}{\hbar}\mathcal{E}_c. \tag{14}$$

Since G and g depend on position and time via the envelope functions $\mathcal{E}_p$ and $\mathcal{E}_c$, the density operator ϱ in the rotating frame is a slowly varying function of z and t.

The propagation of the probe and control fields inside the medium is governed by Maxwell's equations that yield a wave equation for the total electric field $\boldsymbol{E}=\boldsymbol{E}_c+\boldsymbol{E}_p$,

$$\left(\frac{1}{c^2}\partial_t^2 - \Delta\right)\boldsymbol{E} = -\frac{1}{c^2\epsilon_0}\partial_t^2\boldsymbol{P}. \tag{15}$$

The source term on the right-hand side of Eq. (15) comprises the macroscopic polarization $\boldsymbol{P}$ induced by the control and probe fields. For a dilute gas, atom-atom interactions can be neglected such that $\boldsymbol{P}$ can be expressed in terms of the single-atom polarization,

$$\boldsymbol{P} = \mathcal{N}(\boldsymbol{d}_{13}R_{31} + \boldsymbol{d}_{23}R_{32} + \text{c.c.}). \tag{16}$$

In this equation, $\mathcal{N}$ is the mean atomic density of the medium. Note that coherences R_{31} and R_{32} in Eq. (16) are related to the coherences of the density operator ϱ in the rotating frame by

$$R_{31} = \varrho_{31}e^{-i\omega_p(t-z/c)}, \quad R_{32} = \varrho_{32}e^{-i\omega_c(t-z/c)}. \tag{17}$$

In the slowly varying envelope approximation [24] and with Eqs. (1), (2), and (14), the wave Eq. (15) can be cast into the form

$$\left(\partial_z + \frac{1}{c}\partial_t\right)g = i\eta\varrho_{31}, \tag{18a}$$

$$\left(\partial_z + \frac{1}{c}\partial_t\right)G = i\eta\varrho_{32}, \tag{18b}$$

where the coupling constant η is given by

$$\eta = \gamma\frac{3\mathcal{N}\lambda^2}{8\pi}, \tag{19}$$

and λ is the mean wavelength of the atomic transitions $|3\rangle\leftrightarrow|i\rangle(i\in\{1,2\})$. Equation (17) relates the Rabi frequencies g and G of the probe and control fields to the coherences ϱ_{31} and ϱ_{32} of the density operator in the rotating frame. On the other hand, Eq. (11) governs the time evolution of the density operator ϱ in dependence on g and G. The set of Eqs. (11) and (18) represent a system of coupled partial differential equations and have to be solved consistently for given initial and boundary conditions that we specify in Sec. III. Since analytical solutions to the Maxwell-Bloch equations are only known under special conditions [25–27], we pursue a numerical approach.

III. NUMERICAL RESULTS

In this section, numerical solutions to the Maxwell-Bloch equations derived in Sec. II are presented. We begin with a specification of the initial and boundary conditions for the functions ϱ, g, and G. The initial state of the atomic system for $z\in[0,L]$ is given by

$$\varrho(z,t=0) = |1\rangle\langle 1|. \tag{20}$$

Note that this state can be prepared if the atoms are pumped by the control field alone. The initial conditions for the Rabi frequencies of the probe and control fields are

$$g(z,t=0) = 0, \quad G(z,t=0) = G_0, \tag{21}$$

where $z\in[0,L]$ and the parameter G_0 is a constant. If the boundary condition Eq. (3) for the phase-modulated control field at $z=0$ is rewritten in terms of the Rabi frequency G, we obtain [28]

$$G(z=0,t) = G_0\exp[-i\varphi(t)], \tag{22}$$

where $\varphi(t)$ is defined in Eq. (4). In the first step, we consider the case of a continuous probe field that is switched on slowly at $t=0$,

$$g(z=0,t) = g_0\left[1 - \frac{1}{1+(t\gamma)^4/2}\right], \tag{23}$$

and g_0 is a constant parameter. It follows that at $z=0$, g is exactly equal to zero at $t=0$ and increases smoothly until the maximal value of g_0 is reached for $t\gtrsim 5/\gamma$.

In the following, we suppose that the atomic decay rates γ_1 and γ_2 are equal and set as $\gamma_1=\gamma_2=\gamma$. Furthermore, we exchange the variables t and z in Eqs. (11) and (18) with the dimensionless variables,

$$\tau = t\gamma, \quad \zeta = z\eta/\gamma = z\frac{3\mathcal{N}\lambda^2}{8\pi}. \tag{24}$$

It follows that the atomic density $\mathcal{N}$ of the medium enters Eq. (18) via the parameter

$$\mathcal{C} = c\eta/\gamma^2 = \frac{3\mathcal{N}\lambda^2 c}{8\pi\gamma}, \tag{25}$$

which represents the vacuum speed of light in scaled position and time variables. For all numerical integrations, we set $\mathcal{C}=70\times10^3$, which corresponds approximately to the values $\lambda=800$ nm, $\gamma=10^7$ s^{-1}, and $\mathcal{N}=3\times10^{16}$ m^{-3}. We emphasize that the solution to Eqs. (11) and (18) is extremely insensitive with respect to the numerical value of $\mathcal{C}$, provided that realistic cell lengths of a few centimeter are considered.

The numerical integration of Eqs. (11) and (18) is computationally demanding, in particular, because of the phase modulation of the control field. Therefore, we employ two different numerical methods to ensure the reliability of our results.

The first method is based on MATHEMATICA and the implicit differential-algebraic solver (IDA) method option for NDSolve. With this choice, the system of partial differential equations is integrated via the method of lines, and the time

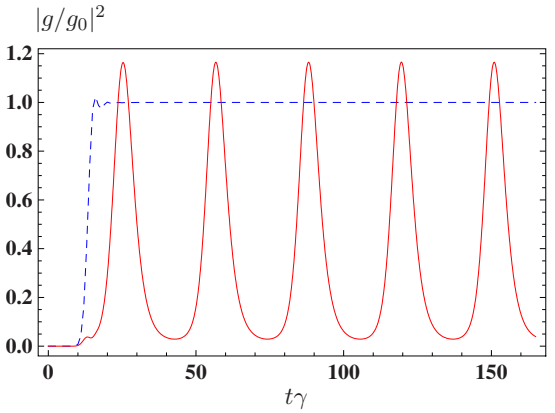

FIG. 2. (Color online) The relative probe field intensity $|g/g_0|^2$ at the boundary $z=L$ for the slowly turned-on probe field in Eq. (23). We set $L=150\gamma/\eta$ which corresponds to a cell length of $L\approx 6.5$ cm for an atomic density $\mathcal{N}=3\times 10^{16}$ m^{-3} and a mean transition wavelength $\lambda=800$ nm. The dashed line demonstrates the EIT phenomenon for the probe field if the phase modulation of the control field is switched off, i.e., $M=0$ and $\Omega=0$ in Eq. (4). The phase modulation of the control field changes the transmitted probe field intensity considerably, as can be seen from the solid line that corresponds to $M=16$ rad and $\Omega=0.1\gamma$. The remaining parameters for both curves are $G_0=\sqrt{15}\gamma$, $g_0=\sqrt{0.1}\gamma$, and $\Delta_p=\Delta_c=0$.

integration is accomplished with an implicit differential-algebraic solver.

The second method consists of the standard approach [13] where the transformation to the comoving frame $\xi=t-z/c$ reduces Eq. (18) to a differential equation with respect to the spacial variable z alone. This equation together with Eq. (11) allows then to propagate the field variables g and G along the z direction.

We find that both numerical methods yield the same results that are presented in Fig. 2. The dashed line shows the expected EIT phenomenon in the absence of phase modulation. Note that the small oscillations around $t\gamma=15$ are due to nonadiabatic processes in the turn-on phase that have been studied in [29,30]. The solid curve corresponds to the phase-modulated control field. A comparison of the two curves clearly demonstrates that the phase modulation changes the optical properties for the probe field dramatically. In the presence of phase modulation, the probe field is not transmitted continuously, but periodically at equidistant points in time, separated by $\Delta T\approx 31.4\gamma^{-1}$. In addition, the maximal intensity at $z=L$ is larger than the intensity of the probe field at $z=0$. Note that the minimal intensity of the probe field is not equal to zero, and this offset persists even if the cell length L is increased.

Next we consider the propagation of a Gaussian probe pulse, which gives rise to the following boundary conditions at $z=L$ [31],

$$g(z=0,t)=g_0\exp[-(t-t_0)^2/(2\sigma_p^2)]. \tag{26}$$

In addition, we assume that the central frequency ω_p is detuned from the two-photon resonance with the control field. The results of the numerical integration are shown in Fig. 3, and demonstrate that the pulse is absorbed without frequency

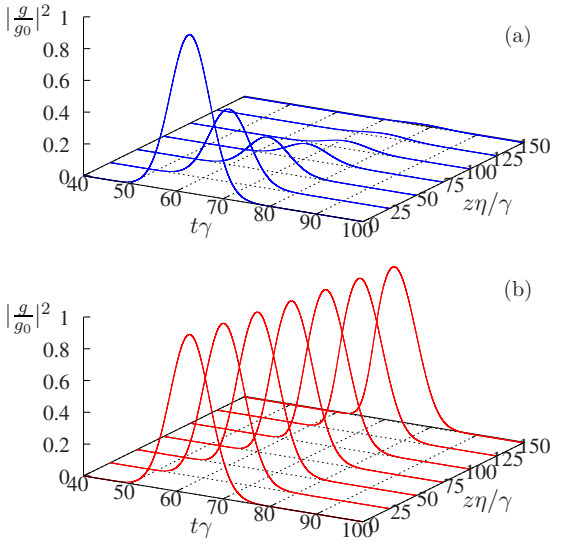

FIG. 3. (Color online) The relative probe field intensity $|g/g_0|^2$ as a function of position and time for the Gaussian probe pulse in Eq. (26) with $t_0=20\pi\gamma^{-1}$ and $\sigma_p=6\gamma^{-1}$. The detuning of the probe pulse and the control field is given by $\Delta_p=1.6\gamma$ and $\Delta_c=0$, respectively, and the maximal Rabi frequencies are $G_0=\sqrt{15}\gamma$ and $g_0=\sqrt{0.1}\gamma$. (a) Since the two-photon resonance condition is not fulfilled, the probe pulse is absorbed in the case of no phase modulation. (b) For the phase modulation parameters $M=16$ rad and $\Omega=0.1\gamma$, the probe pulse is transmitted almost without losses.

modulation of the control field [Fig. 3(a)] as expected. On the contrary, Fig. 3(b) shows that the probe pulse is transmitted through the medium almost without losses if the phase modulation is switched on. Note that this result depends on the time t_0 at which the probe pulse maximum reaches the boundary $z=0$. We find that the medium becomes transparent for the probe pulse for $t_0=20\pi\gamma^{-1}$ and also at integer multiples of t_0. At different times, the medium is opaque and the probe pulse is absorbed. A discussion of the numerical results based on a theoretical model is provided in Sec. IV.

IV. THEORETICAL ANALYSIS

The aim of this section is to provide a theoretical explanation for the numerical results presented in Sec. III. To this end, we assume that the control field is much larger than the probe field intensity and present a model that is linear in the probe field Rabi frequency g.

A. Linear theory

The starting point of our calculation is the master equation (11) with the Hamiltonian in Eq. (12). In Sec. II, the phase modulation of the control field was taken into account via the boundary condition at $z=0$, see Eq. (3). Here we neglect the reaction of the medium on the control field, such that the phase-modulated control field Rabi frequency can be written as [32]

$$G(z,t)=G_0e^{-i\varphi(t)}. \tag{27}$$

This simplification allows us to replace the Hamiltonian H' in Eq. (12) by

$$H' = \hbar\Delta_p|1\rangle\langle 1| + \hbar\Delta_c|2\rangle\langle 2| - \hbar(g|3\rangle\langle 1| + G_0 e^{-i\varphi(t)}|3\rangle\langle 2| + \text{H.c.}). \tag{28}$$

The generic way to solve the master equation with this Hamiltonian is to decompose the time-dependent phase factor $\exp[-i\varphi(t)]$ via Eq. (5) into its frequency components and to perform a Floquet decomposition [33] of the density operator ϱ. On the contrary, here we pursue a different approach that allows us to determine the solution of the master equation in leading order in the small parameter g/G_0 directly. Note that this is only possible since the intensity of the control field is time independent, see Sec. II. In order to facilitate the calculation and the physical interpretation of the result, we introduce the unitary transformation,

$$U = \exp[-i\varphi(t)|2\rangle\langle 2|]. \tag{29}$$

The master equation (11) for the transformed density operator $\sigma = U\varrho U^\dagger$ then reads as

$$\partial_t \sigma = -\frac{i}{\hbar}[H_0(t) + H_p, \sigma] + \mathcal{L}_\gamma \sigma, \tag{30}$$

where H_p describes the interaction of the probe field with the $|3\rangle \leftrightarrow |1\rangle$ transition,

$$H_p = -\hbar g|3\rangle\langle 1| + \text{H.c.}. \tag{31}$$

The Hamiltonian $H_0(t)$ is given by

$$H_0(t) = \hbar[\Delta_p|1\rangle\langle 1| + \delta_c(t)|2\rangle\langle 2| - (G_0|3\rangle\langle 2| + \text{H.c.})], \tag{32}$$

and the time-dependent function $\delta_c(t)$ is

$$\delta_c(t) = \Delta_c + \partial_t\varphi(t) = \Delta_c + M\Omega\cos(\Omega t). \tag{33}$$

Note that it is the temporal derivative of the phase modulation function φ that enters Eq. (33). Since frequency is the temporal derivative of the total phase, the phase modulation according to Eqs. (3) and (4) appears as a modulation of the control field frequency ω_c with amplitude $M\Omega$ in the rotating frame defined by Eq. (29). It follows that $\delta_c(t)$ is the time-dependent detuning of the control field with the $|3\rangle \leftrightarrow |2\rangle$ transition.

Since we are interested in the linear response of the atoms to the probe field, we expand the density operator as $\sigma = \sigma_0 + \sigma_p$, where σ_p is linear in the probe field. If only terms up to first order with respect to g are retained in Eq. (11), we obtain the two coupled equations,

$$\partial_t \sigma_0 = \mathcal{L}_0 \sigma_0, \tag{34a}$$

$$\partial_t \sigma_p = \mathcal{L}_0 \sigma_p - \frac{i}{\hbar}[H_p, \sigma_0], \tag{34b}$$

and the superoperator $\mathcal{L}_0$ is defined as

$$\mathcal{L}_0(\cdot) = -\frac{i}{\hbar}[H_0(t), \cdot] + \mathcal{L}_\gamma(\cdot). \tag{35}$$

Here the centered dot denotes the position of the argument of $\mathcal{L}_0$. The zeroth order Eq. (34a) describes the interaction of the atom with the control field to all orders, and Eq. (34b) determines the influence of the probe field to first order in g. The initial condition in Eq. (20) is at the same time the steady-state solution $\sigma_0 = |1\rangle\langle 1|$ of Eq. (34a), and thus it remains to solve Eq. (34b). To this end, we decompose the probe field into its frequency components,

$$g(z,t) = \int_{-\infty}^{\infty} \tilde{g}(z,\omega) e^{-i\omega t} d\omega. \tag{36}$$

If $\tilde{\sigma}_p(t,\omega)$ denotes the solution of Eq. (34b) for a single Fourier component ω,

$$\partial_t \tilde{\sigma}_p = \mathcal{L}_0 \tilde{\sigma}_p - i\tilde{g} e^{-i\omega t}|3\rangle\langle 1| + i\tilde{g}^* e^{i\omega t}|1\rangle\langle 3|, \tag{37}$$

the linearity of Eq. (37) with respect to $\tilde{g}$ implies that

$$\sigma_p(z,t) = \int_{-\infty}^{\infty} \tilde{\sigma}_p(\omega,t) d\omega \tag{38}$$

is a solution of Eq. (34b). The propagation Eq. (18a) for the probe field involves the coherence ϱ_{31}. Since the unitary transformation U in Eq. (29) does not act on the $|1\rangle \leftrightarrow |3\rangle$ transition, we have $\varrho_{31} = [\sigma_p]_{31}$ and thus

$$\varrho_{31}(z,t) = \int_{-\infty}^{\infty} f(\omega,t)\tilde{g}(z,\omega) e^{-i\omega t} d\omega, \tag{39}$$

where $f(\omega,t) = [\tilde{\sigma}_p(\omega,t)]_{31} e^{i\omega t}/\tilde{g}(z,\omega)$.

The following explanation of the system behavior as well as quantitative calculations in this section are based on $f(\omega,t)$. This function is periodic in time with period $2\pi/\Omega$ when the system has reached a quasisteady state such that the solution of Eq. (37) does not depend on the initial conditions. For all numerical calculations in Sec. IV C, we determine $f(\omega,t)$ by a numerical integration of Eq. (37).

An approximate solution of f can be found if the time dependence of $\mathcal{L}_0$ in Eq. (37) is ignored. In this case, we find

$$f(\omega,t) \approx -\frac{[\delta_p(\omega) - \delta_c(t)]}{[\delta_p(\omega) - \delta_c(t)][i\gamma + \delta_p(\omega)] - |G_0|^2}, \tag{40}$$

and $\delta_p(\omega) = (\omega_p + \omega) - \omega_{31}$ is the detuning of the probe field frequency component $(\omega_p + \omega)$ with the $|1\rangle \leftrightarrow |3\rangle$ transition. This approximation describes all essential features of the function f if the modulation frequency Ω is sufficiently small, and this is the case for the parameters we chose.

An interpretation of the function f can be found if the polarization induced on the $|3\rangle \leftrightarrow |1\rangle$ transition is considered. According to Eqs. (16) and (39), we have

$$\boldsymbol{P}_{3\leftrightarrow 1} = \epsilon_0 \frac{\boldsymbol{d}_{13}}{|\boldsymbol{d}_{13}|} \int_{-\infty}^{\infty} \chi(\omega,t)\tilde{\mathcal{E}}_p(z,\omega) e^{-i\omega t} d\omega e^{-i\omega_p(t-z/c)} + \text{c.c.}, \tag{41}$$

where $\tilde{\mathcal{E}}_p(z,\omega)$ is the Fourier transform of $\mathcal{E}_p(z,t)$ [see Eq. (1b)], and the function

$$\chi(\omega,t) = \frac{2\eta}{k_p} f(\omega,t) \tag{42}$$

can be regarded as the *time-dependent* susceptibility of the medium. Figures 4(b)–4(d) show the real and imaginary

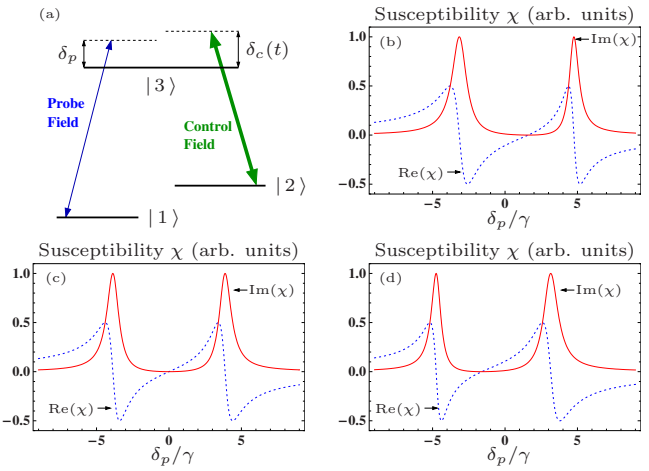

FIG. 4. (Color online) Level scheme with the detuning δ_p of the probe field and the time-dependent detuning $\delta_c(t)$ of the control field. Subfigures (b), (c), and (d) show the real (dotted line) and imaginary (solid line) parts of the time-dependent susceptibility χ in Eq. (42) and correspond to time $t_b=0$, $t_c=\pi/(\Omega 2)$, and $t_d=\pi/\Omega$, respectively. Note that χ is periodic with time $T=2\pi/\Omega$.

parts of $\chi(\omega,t)$ at different times. It follows that the transparency window oscillates in frequency space with period $2\pi/\Omega$. This behavior is due to the phase modulation of the control field that causes the time-dependent detuning $\delta_c(t)$. In Sec. IV B, we will discuss the physical meaning of this time-dependent susceptibility and demonstrate that it allows us to understand the essential features of the system. If the modulation frequency approaches zero, i.e., $\Omega\to 0$, χ is time independent and Eq. (42) reduces to the standard result for the susceptibility in an EIT medium [24].

We aim at a solution of the propagation Eq. (18a) by Fourier transform with respect to time. However, we stress that f in Eq. (40) depends explicitly on time, and thus the integral in Eq. (39) cannot be interpreted as the Fourier decomposition of the coherence $\varrho_{31}(z,t)$. However, the required Fourier representation is readily obtained if the periodic function f is expanded in a Fourier series,

$$f(\omega,t)=\sum_{n=-\infty}^{\infty} f_n(\omega)e^{in\Omega t}, \tag{43}$$

where the coefficients f_n are determined by

$$f_n(\omega)=\frac{\Omega}{2\pi}\int_0^{2\pi/\Omega} f(\omega,t)e^{-in\Omega t}dt. \tag{44}$$

It follows that the Fourier transform of Eq. (39) with respect to time is

$$\frac{1}{2\pi}\int_{-\infty}^{\infty}\varrho_{31}(z,t)e^{i\omega t}dt=\sum_{n=-\infty}^{\infty} f_n(\omega+n\Omega)\tilde{g}(z,\omega+n\Omega). \tag{45}$$

In frequency space, Eq. (18b) can thus be written as

$$(-i\omega/c+\partial_z)\tilde{g}(z,\omega)=i\eta\sum_{n=-\infty}^{\infty} f_n(\omega+n\Omega)\tilde{g}(z,\omega+n\Omega). \tag{46}$$

Before we continue with the solution of the propagation equation, we establish a simple physical picture that allows us to understand the essential features of the numerical results presented in Sec. III.

B. Physical explanation

The aim of this section is to illustrate the physical meaning of the time-dependent susceptibility χ. In the first step, we analyze the situation where the phase modulation of the control field is switched off, which implies that the susceptibility is time independent, $\chi(\omega,t)\equiv\chi_0(\omega)$. In this case, the propagation Eq. (46) reduces to

$$(-i\omega/c+\partial_z)\tilde{g}(z,\omega)=i\frac{k_p}{2}\chi_0(\omega)\tilde{g}(z,\omega). \tag{47}$$

This equation can be immediately solved and yields the well-known solution [24] of the pulse propagation problem in a medium with a linear susceptibility,

$$g(z,t)=\int_{-\infty}^{\infty}\exp\{i[\omega/c+\chi_0(\omega)k_p/2]z-i\omega t\}\tilde{g}(0,\omega)d\omega. \tag{48}$$

The action of the medium on the probe field is thus determined by the susceptibility χ_0 or equivalently the refractive index $n=1+\chi_0(\omega)/2$. Our analysis below Eq. (40) demonstrates that such a simple solution of the pulse propagation problem is not possible if f and hence χ is time dependent.

However, it follows from Eqs. (18a) and (39) that a relation similar to Eq. (48) holds even for a time-dependent susceptibility if an infinitesimal increment δz is considered,

$$\begin{aligned} g(z+\delta z,t)&\approx g(z,t)+\partial_z g(z,t)\delta z\\ &\approx\int_{-\infty}^{\infty}\exp\{i[\omega/c+\chi(\omega,t)k_p/2]\delta z\\ &\quad -i\omega t\}\tilde{g}(z,\omega)d\omega. \end{aligned} \tag{49}$$

Note that in the second line we assumed that the inequality $|[\omega/c+\chi(\omega,t)k_p/2]\delta z|\ll 1$ holds, which is always the case for sufficiently small δz. Equation (49) means that $\chi(\omega,t)$ can be employed to propagate the probe field amplitude from z to $z+\delta z$ for an infinitesimal increment δz. It is reasonable to expect that this result also allows us to estimate the probe field for small but not infinitesimal increments δz. Since the Fourier components of the probe field at the boundary $z=0$ are known, Eq. (49) enables us to estimate the influence of the first section of the medium on the probe field via the susceptibility $\chi(\omega,t)$. Since the phase modulation gives rise to a time-dependent control field detuning $\delta_c(t)$, the probe field frequency that fulfills the two-photon resonance condition also depends on time. Therefore, the transparency window oscillates in time, see Fig. 4. In the following, we show

that this intuitive picture allows us to explain the essential features of the numerical results in Sec. III.

First we discuss the sequence of pulses that arrive at $z=L$ if a continuous probe field is applied to the phase-modulated medium, see Fig. 2. At the boundary $z=0$, the Fourier spectrum $\tilde{g}(z,\omega)$ of the continuous probe field consists of a single peak at $\omega=0$. Since the probe field is assumed to be resonant, Eqs. (40) and (42) imply that the imaginary part of $\chi(\omega=0,t_n)$ vanishes if the time-dependent control field detuning satisfies $\delta_c(t_n)=0$. This relation holds at times $t_n=\pi/(2\Omega)+n\pi/\Omega$, where $n\in\mathbb{N}$. At these times, Eq. (49) predicts that the probe field can enter the medium; at other times it is absorbed. Exactly this periodic change from transparency to opacity generates the sequence of pulses that is observed at $z=L$. Since the time difference $t_{n+1}-t_n$ between two transparency periods is π/Ω, it is expected that the time separation between the pulses is given by π/Ω. For the particular choice of $\Omega=0.1\gamma$ as in Fig. 2 we obtain $t_{n+1}-t_n\approx 31.4\gamma^{-1}$, which is in excellent agreement with the numerical result (see Sec. III).

Next we turn to Fig. 3, where it is shown that a detuned probe pulse with $\Delta_p=1.6\gamma$ can propagate through the medium virtually without losses only if the phase modulation is turned on and if the pulse maximum arrives at certain times at $z=0$. These results can be explained as follows. For the parameters chosen in Fig. 3, the imaginary part of $\chi(\omega=0,t_n)$ vanishes at times $t_n=n2\pi/\Omega=n20\pi\gamma^{-1}$ $(n\in\mathbb{N})$ where the time-dependent control field detuning satisfies $\delta_c(t_n)=\Delta_p$, see Eqs. (40) and (42). Since the pulse maximum arrives at $t_1=20\pi\gamma^{-1}$, Eq. (49) shows that the probe pulse can enter the medium. If the pulse maximum arrives at other times than t_n, the imaginary part of χ is nonzero and the pulse is absorbed. Note that we also considered different values of the probe field detuning Δ_p and found that the times at which the medium becomes transparent can be predicted reliably with similar arguments.

In the above discussion, we assumed that the Fourier components of the probe field are sharply peaked around the central frequency ω_p of the probe field. As we will show in Sec. IV C, the phase modulation of the control field will considerably broaden the frequency spectrum of the probe pulse as it propagates through the medium. This process is the physical reason why Eq. (49) holds only for small propagation lengths δz during which the broadening of the pulse in frequency space is negligible.

C. Probe field reconstruction

Here we demonstrate that the linear theory established in Sec. IV A allows us to recover the numerical results obtained in Sec. III. Maxwell's equation (46) for the probe field in Fourier space implies that the Fourier component $\tilde{g}(z,\omega)$ is coupled to the components $\tilde{g}(z,\omega+n\Omega)$ via the coefficients f_n. These coefficients correspond to the Fourier series expansion of the periodic function f in Eq. (44). Fortunately, this series converges quite rapidly for the parameters we chose such that only a few coefficients have to be taken into account. In addition, it is reasonable to assume that the Fourier spectrum of the probe field has a finite width. These two simplifying assumptions can be summarized as follows:

$$f_n\approx 0,\quad |n|>Q\in\mathbb{N}, \tag{50a}$$

$$\tilde{g}(z,\omega)\approx 0,\quad |\omega|>\omega_{\max}. \tag{50b}$$

In order to obtain the probe field Fourier components at a given position z, we introduce the vector $\boldsymbol{y}^{(\omega)}$ with the $2K+1$ components,

$$\boldsymbol{y}_j^{(\omega)}(z)=\tilde{g}(z,\omega-K\Omega+j\Omega),\quad j\in\{0,\ldots,2K\}. \tag{51}$$

The value of K should be chosen such that all nonzero components of $\tilde{g}$ are included in $\boldsymbol{y}^{(\omega)}$. With the help of Eq. (46), one derives the differential equation,

$$\partial_z\boldsymbol{y}^{(\omega)}=M(\omega)\boldsymbol{y}^{(\omega)}, \tag{52}$$

where $M(\omega)$ is a $(2K+1)\times(2K+1)$ matrix that will not be given here. The solution of Eq. (52) is given by $\boldsymbol{y}^{(\omega)}(z)=\exp[M(\omega)z]\boldsymbol{y}^{(\omega)}(z=0)$ and can be determined numerically. This procedure allows us to obtain the probe field Fourier components contained in the vector $\boldsymbol{y}^{(\omega)}(z)$ from the Fourier components at the boundary $z=0$.

First we assume that a continuous probe field is applied to the medium. In this case, the probe field Fourier components at $z=0$ are given by a delta function centered at $\omega=0$. We find that the Fourier spectrum for $z>0$ is discrete such that the probe field can be written as

$$g(z,t)=\sum_{j=0}^{2K}\tilde{g}_j(z)\exp[-i\Omega(j-K)t]. \tag{53}$$

For the evaluation of the Fourier components $\tilde{g}_j(z)$, we chose $Q=4$ and $\omega_{\max}=30\ \Omega$ in Eq. (50), and their absolute values $|\tilde{g}_j(z)|$ are shown in Fig. 5(a). The dots in Fig. 5(b) represent the relative probe field intensity according to Eq. (53) for the same parameters than in Fig. 2. It can be seen that the results obtained from the linear theory are in very good agreement with the numerical integration of Maxwell-Bloch equations that yields the solid line in Fig. 5(b). The deviations for $t\gamma<15$ are due to the fact that we did not take into account the turn-on process of the probe field in Eq. (53).

Next we consider the probe pulse in Eq. (26) and solve Eq. (52) for different values of ω with $Q=6$ and $\omega_{\max}=30\ \Omega$ [see Eq. (50)]. This procedure allows us to generate $\tilde{g}(z,\omega)$ on a dense grid of frequencies, and the absolute values $|\tilde{g}(z,\omega)|$ are presented in Fig. 6(a) for several values of z. It can be seen that the Fourier components broaden and acquire a shift of their central frequency as the probe pulse propagates through the medium. Figure 6(b) shows the relative probe field intensity for the same parameters than in Fig. 3. The dotted line is obtained by the evaluation of Eq. (36) via a discrete Fourier transform, and the solid line corresponds to the numerical integration of Maxwell-Bloch equations. As for the case of a continuous probe field, we obtain excellent agreement between the linear theory and the numerical findings.

V. DISCUSSION AND SUMMARY

In this paper, we investigated the phenomenon of electromagnetically induced transparency (EIT) for a weak probe

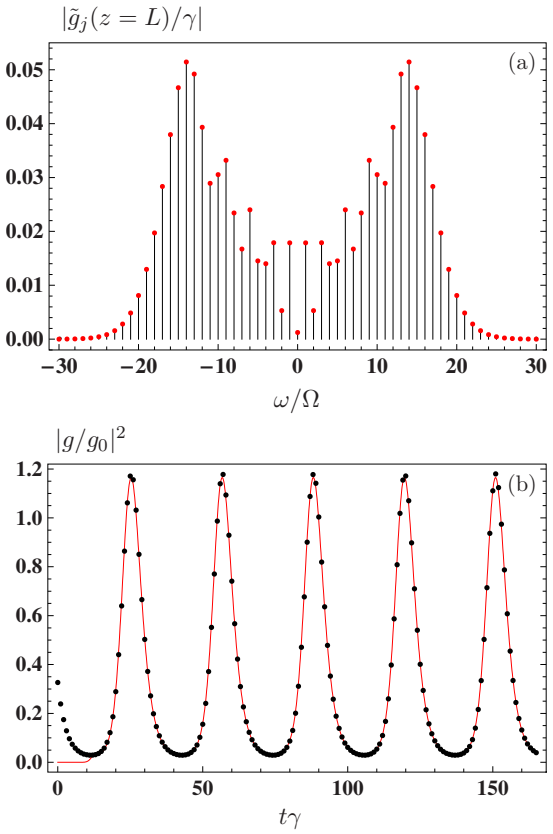

FIG. 5. (Color online) (a) Discrete probe field Fourier spectrum at $L=150\gamma/\eta$ if a continuous probe field is applied to the medium. Since the Fourier spectrum at $z=0$ corresponds to a single delta peak, the phase-modulated control field results in a broadening of the probe field. (b) Relative probe field intensity at $L=150\gamma/\eta$ for the same parameters than in Fig. 2. The dotted line corresponds to the result of the linear theory in Eq. (53), and the solid line results from a numerical integration of Maxwell-Bloch equations.

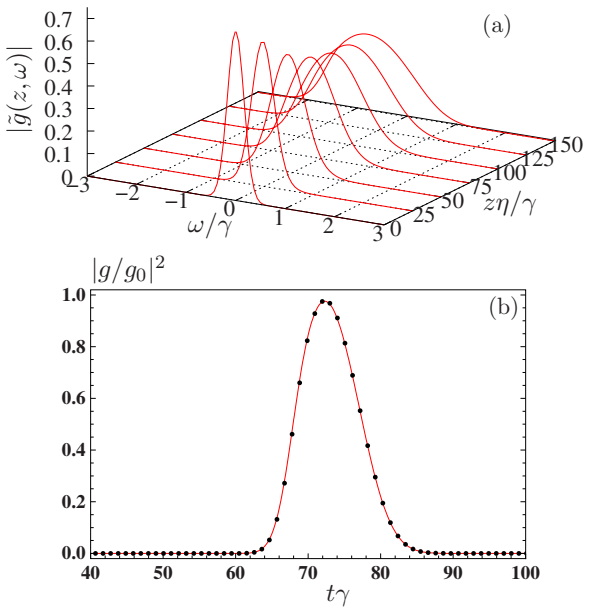

FIG. 6. (Color online) (a) The absolute value of the (dimensionless) Fourier components $|\tilde{g}(z,\omega)|$ at different positions z if a Gaussian probe pulse is sent into the medium. The Fourier spectrum of the probe field broadens and the central frequency of the pulse is shifted to smaller frequencies. (b) Relative probe field intensity at $L=150\gamma/\eta$ for the same parameters than in Fig. 3. The dotted line corresponds to the linear theory and was generated by the evaluation of Eq. (36) via a discrete Fourier transform. The solid line results from a numerical integration of Maxwell-Bloch equations.

field in the presence of a phase-modulated control field. By a numerical integration of Maxwell-Bloch equations, we found that the phase modulation changes the dispersive properties of the medium considerably.

If a continuous probe field is applied to the medium, we have shown that the medium results in the generation of a train of pulses that arrives at the output of the gas cell. The peak intensity of the output pulses exceeds the intensity of the input field by almost 20%, and the intensity between successive pulse drops to 3% of the incoming field. In practice, this feature of our system could be employed to generate smooth pulses from a cw laser field. Note that a time-dependent variation in the probe field transmission was also achieved [34] in an EIT experiment based on an atomic double-Λ system. In contrast to the present scheme, however, the transparency of the medium in [34] is determined by the instantaneous phase difference of the involved laser fields in a closed-loop configuration. In addition, other mechanisms that allow us to reshape the probe pulse in an EIT system have been studied in [35].

A major result of this paper is that the medium supports the propagation of probe pulses with different central frequencies at different times. This result is in striking contrast to the standard EIT setup, where the medium is only transparent for a single probe field frequency that is determined by the two-photon resonance condition. It follows that our system enhances the potential of EIT media for the purpose of signal processing since the medium acts like a frequency selective switch. Subject to the central frequency of the probe pulse and its time of arrival, the pulse is either transmitted or absorbed.

In order to explain our results, we established a theoretical model that is linear in the probe field Rabi frequency. We found that the phase modulation of the control field gives rise to a time-dependent susceptibility that allows us to understand the behavior of the medium intuitively. In essence, the phase modulation is effectively a frequency modulation of the control field. Therefore, the frequency component that fulfills the two-photon resonance condition also changes with time, and hence the transparency window changes its position in frequency space periodically in time. This physical picture is valid, provided that the analytical expression for the time-dependent susceptibility in Eq. (40) is a good approximation of the corresponding numerical result. A numerical analysis shows that this requires that the parameters of the phase modulation are sufficiently small, i.e., $M\Omega$ should be of the order of the decay rate γ of the upper state and $\Omega \ll \gamma$.

We also studied the influence of the phase modulation on the probe field in the frequency domain. To this end, we expanded the time-dependent susceptibility in a Fourier se-

ries and solved the propagation equation for the probe field in Fourier space. This procedure reveals that the phase modulation causes a coupling between different probe-field Fourier components. As the probe field propagates through the medium, this coupling results in a broadening of the pulse in the frequency domain. Moreover, we find that the central frequency of a probe pulse experiences a shift if the central frequencies of the probe and control fields do not satisfy the two-photon resonance condition. For the parameters we chose, the detuning of the probe pulse at the entrance of the medium is positive and the control field is in resonance. As the pulse propagates through the medium, the Fourier components of the probe field experience a shift toward smaller frequencies, see Fig. 6(a). In general, this means that the central frequency of the probe field is shifted such that it gets into two-photon resonance with the central frequency of the control field. Despite the broadening of the Fourier components, the shape of the probe pulse in the time domain remains almost unchanged. Therefore, this effect can be employed to shift the frequency of a pulse almost without distortion of its shape. Note that the maximal frequency shift that the probe pulse can acquire until it is in two-photon resonance with the central frequency of the control field is given by $M\Omega$, i.e., half the range of the control field frequency variation. Due to the constraints that apply to the parameters M and Ω, the frequency shift can be at most of the order of the decay rate γ of the excited state.

Finally, the influence of the medium on the frequency components of the probe field demonstrates that the system seeks to maximize transparency. This is related to the phenomenon of pulse matching [36–38], where the medium renders itself transparent by the generation of matched Fourier components. For the system under consideration, perfect pulse matching corresponds to a phase-modulated continuous probe field. Since the medium is passive, a continuous wave cannot be created from a pulse for energetic reasons, and thus perfect pulse matching never occurs if a probe pulse is applied to the medium. The situation is different in the case of a continuous probe field, where we find that a fraction of 3% of the incoming intensity is transferred into a perfect trapping state.

ACKNOWLEDGMENT

M.K. thanks M. D. Lukin for helpful discussions.

[1] S. E. Harris, J. E. Field, and A. Imamoğlu, Phys. Rev. Lett. **64**, 1107 (1990).
[2] K.-J. Boller, A. Imamoğlu, and S. E. Harris, Phys. Rev. Lett. **66** (7), 2593 (1991).
[3] S. E. Harris, Phys. Today **50**, 36 (1997).
[4] M. Fleischhauer, A. Imamoğlu, and J. P. Marangos, Rev. Mod. Phys. **77**, 633 (2005).
[5] M. D. Lukin, Rev. Mod. Phys. **75**, 457 (2003).
[6] L. V. Hau, S. E. Harris, Z. Dutton, and C. Behroozi, Nature (London) **397**, 594 (1999).
[7] M. M. Kash, V. A. Sautenkov, A. S. Zibrov, L. Hollberg, G. R. Welch, M. D. Lukin, Y. Rostovtsev, E. S. Fry, and M. O. Scully, Phys. Rev. Lett. **82**, 5229 (1999).
[8] D. Budker, D. F. Kimball, S. M. Rochester, and V. V. Yashchuk, Phys. Rev. Lett. **83**, 1767 (1999).
[9] C. Liu, Z. Dutton, C. H. Behroozi, and L. V. Hau, Nature (London) **409**, 490 (2001).
[10] D. F. Phillips, A. Fleischhauer, A. Mair, R. L. Walsworth, and M. D. Lukin, Phys. Rev. Lett. **86**, 783 (2001).
[11] M. Fleischhauer and M. D. Lukin, Phys. Rev. Lett. **84**, 5094 (2000).
[12] M. Fleischhauer and M. D. Lukin, Phys. Rev. A **65**, 022314 (2002).
[13] T. N. Dey and G. S. Agarwal, Phys. Rev. A **67**, 033813 (2003).
[14] H. Schmidt and A. Imamoğlu, Opt. Lett. **21**, 1936 (1996).
[15] S. E. Harris and Y. Yamamoto, Phys. Rev. Lett. **81**, 3611 (1998).
[16] M. D. Lukin and A. Imamoğlu, Phys. Rev. Lett. **84**, 1419 (2000).
[17] H. Kang and Y. Zhu, Phys. Rev. Lett. **91**, 093601 (2003).
[18] D. A. Braje, V. Balic, S. Goda, G. Y. Yin, and S. E. Harris, Phys. Rev. Lett. **93**, 183601 (2004).
[19] M. Bashkansky, G. Beadie, Z. Dutton, F. K. Fatemi, J. Reintjes, and M. Steiner, Phys. Rev. A **72**, 033819 (2005).
[20] Q. Sun, Y. V. Rostovtsev, J. P. Dowling, M. O. Scully, and M. S. Zubairy, Phys. Rev. A **72**, 031802(R) (2005).
[21] Z. Deng, D. K. Qing, P. Hemmer, C. H. Raymond Ooi, M. S. Zubairy, and M. O. Scully, Phys. Rev. Lett. **96**, 023602 (2006).
[22] Z. Dutton, M. Bashkansky, M. Steiner, and J. Reintjes, Opt. Express **14**, 4978 (2006).
[23] D. D. Yavuz, Phys. Rev. A **75**, 031801(R) (2007).
[24] M. O. Scully and M. S. Zubairy, *Quantum Optics* (Cambridge University Press, Cambridge, 1997).
[25] R. Grobe, F. T. Hioe, and J. H. Eberly, Phys. Rev. Lett. **73**, 3183 (1994).
[26] A. Rahman and J. H. Eberly, Phys. Rev. A **58**, R805 (1998).
[27] G. Nikoghosyan and G. Grigoryan, Phys. Rev. A **72**, 043814 (2005).
[28] Note that the initial and boundary conditions for G are consistent since $\varphi(t=0)=0$.
[29] A. D. Greentree, T. B. Smith, S. R. de Echaniz, A. V. Durrant, J. P. Marangos, D. M. Segal, and J. A. Vaccaro, Phys. Rev. A **65**, 053802 (2002).
[30] S. R. de Echaniz, A. D. Greentree, A. V. Durrant, D. M. Segal, J. P. Marangos, and J. A. Vaccaro, Phys. Rev. A **64**, 055801 (2001).
[31] To enforce the consistency of the initial and boundary conditions for g, we suppressed the tail of the Gaussian envelope such that $g(z=0,t=0)=0$ holds exactly.
[32] To be consistent with Maxwell's equations, the argument of $\varphi(t)$ should be replaced by the retarded time $t-z/c$. Since retardation effects are small for realistic probe lengths, we suppress this point.

[33] Z. Ficek and S. Swain, *Quantum Interference and Coherence* (Springer, New York, 2005).
[34] E. A. Korsunsky, N. Leinfellner, A. Huss, S. Baluschev, and L. Windholz, Phys. Rev. A **59**, 2302 (1999).
[35] R. Buffa, S. Cavalieri, and M. V. Tognetti, Phys. Rev. A **69**, 033815 (2004).
[36] S. E. Harris, Phys. Rev. Lett. **70**, 552 (1993).
[37] S. E. Harris, Phys. Rev. Lett. **72**, 52 (1994).
[38] M. Fleischhauer, Phys. Rev. Lett. **72**, 989 (1994).